LASER INTERFEROMETER GRAVITATIONAL WAVE OBSERVATORY
- LIGO -
==========
LIGO SCIENTIFIC COLLABORATION

Technical Note	**LIGO-T1500188–v1**	2015/06/04

Active wavefront control in and beyond Advanced LIGO

A. F. Brooks, R. X. Adhikari, S. Ballmer, L. Barsotti, P. Fulda, A. Perreca, D. Ottaway

Distribution of this document:

LIGO Scientific Collaboration

California Institute of Technology
LIGO Project, MS 18-34
Pasadena, CA 91125
Phone (626) 395-2129
Fax (626) 304-9834
E-mail: info@ligo.caltech.edu

Massachusetts Institute of Technology
LIGO Project, Room NW22-295
Cambridge, MA 02139
Phone (617) 253-4824
Fax (617) 253-7014
E-mail: info@ligo.mit.edu

LIGO Hanford Observatory
Route 10, Mile Marker 2
Richland, WA 99352
Phone (509) 372-8106
Fax (509) 372-8137
E-mail: info@ligo.caltech.edu

LIGO Livingston Observatory
19100 LIGO Lane
Livingston, LA 70754
Phone (225) 686-3100
Fax (225) 686-7189
E-mail: info@ligo.caltech.edu

http://www.ligo.org/

Contents

1 Introduction

The purpose of this document is to describe the development of active wavefront control (AWC) in Advanced LIGO and beyond. We will:

- Review, in section 2, the requirements for wavefront matching at different interfaces within the interferometer. We also identify areas where the requirements on wavefront matching are lacking and need to be actively researched, and determine the required ranges for actuators that can be used to correct mismatches.
- Review, in section 3, possible error signals (and sensors) for sensing mode-matching between different interfaces. We also identify interfaces for which we do not yet have well defined error signals and suggest directions for active research into these areas.
- Compare, in section 4, different possible actuation technologies. We stop short of prescribing particular actuator technologies as definite solutions to future AWC systems in this document, however.
- Review, in section 5, the modeling approach for the various aspects of AWC development.
- Review, in section 6, potential LSC partner institutions, with a view to distributing the research and development tasks between the involved institutions.
- Provide, in section 7, a timeline for completion of the R&D tasks prescribed in this whitepaper.
- Review, in section 8, the current TCS as implemented in aLIGO.

The purpose of this document is to be a white-paper to guide wavefront control R&D for the coming months and years. It is designed to be a living document that can be updated as new information becomes available from the interferometer sites and from around the LVC.

2 Active Wavefront Control Requirements

In order to guide the R&D on the implementation of active wavefront control for aLIGO and beyond, it is first necessary to define requirements for what the subsystem must achieve. The aLIGO interferometers include many interfaces between optical cavities, and upgraded detectors are likely to include several more. Mode mismatches and higher-order wavefront mismatches may be expected to occur at each of these interfaces. However, the level of tolerable mismatch varies dramatically over the range of interfaces, as does the expected time dependence of these mismatches. For example, we expect much tighter constraints on the mismatch between squeezer (SQZ) and filter cavity (FC) than between input mode cleaner (IMC) and power recycling cavity (PRC). On the other hand the mode matching between SQZ and FC is not expected to be time dependent, whereas transient thermal processes in the ITMs (and other optics) are expected to cause time dependence in the IMC to PRC matching.

For these reasons, the requirements for wavefront matching at each interface should be evaluated in terms of the following quantities:

- Tolerable wavefront mismatch (size and quadrature[1]).
- Expected static mismatch (size and quadrature).
- Expected time dependent mismatch (size, quadrature and time constant).

The tolerable wavefront mismatch can be compared with the expected total mismatch (static and time dependent) for each interface to first of all determine whether AWC is required for that interface. If the expected total mismatch is greater than the tolerable mismatch, clearly AWC will be required in some form. The time dependent part of the expected mismatch can then be compared with the tolerable mismatch in order to determine whether online closed loop AWC is required for that interface, or whether static one-off corrections are sufficient. This is likely to inform the choice of error signal for the interface (see section 3), as well as possibly the choice of actuator (see section 4). The difference between tolerable mismatch and expected mismatch will inform the required actuation range and quadrature of the actuator.

For further discussion of AWC requirements we divide the IFO into four main regions. There is some overlap between these, but they are:

[1] Quadrature of wavefront mismatch here refers to the type of mismatch between eigenmodes of two cavities sharing an interface: in terms of a simple spherical mode mismatch this equates to the distribution of the mismatch between waist location mismatch and waist size mismatch, or any other pair of orthogonal beam parameters. The term quadrature is appropriate because different types of mode mismatches are well described by the *phase* of the coupling coefficient between the TEM_{00} mode and the HG_{20}+HG_{02} modes (or equivalently the LG_{10} mode).

1. Input region: maximize *coupling* of laser power to IFO
   (a) Pre-stabilized laser (PSL) to pre-mode cleaner (PMC).
   (b) PMC to input mode cleaner (IMC).
   (c) IMC to power-recycling cavity (PRC).
2. Dual recycled Michelson interferometer (DRMI): maximize *efficiency* of power-recycling and signal recycling and control the *interferometer response*.
   (a) PRC to ARMS.
   (b) Signal recycling cavity (SRC) to ARMS.
3. Thermal compensation system (TCS): minimize *thermal effects* in the test masses and the associated problems they cause in the interferometer, such as increasing the *contrast defect*.
   (a) X-ARM to Y-ARM.
   (b) PRX to PRY.
   (c) SRX to SRY.
4. Output region: maximize mode-matching for *squeezing*.
   (a) SRC to output mode cleaner (OMC).
   (b) Squeezed beam (SQZ) to filter cavity (FC).
   (c) FC to SRC.

2.1 Input AWC

Improving mode-matching on the input side of the interferometer improves the efficiency of power coupled to the IFO (therefore allowing for a lower shot-noise limit) and helps to avoid saturation of the REFL detectors. Mode mismatch on the input side is also likely to lead to increased coupling of technical noise sources to REFL sensors, which are nominally prescribed for sensing CARM and SRCL length degrees of freedom.

We require a total throughput of 75% in the IO (125 W out of 160 W in the TEM_{00} mode out of the PSL). We also require less than 5% in higher order modes incident on the PRM. The common understanding is that this means $> 95\%$ mode matching into the common arm cavity mode through the PRC.

2.2 DRMI AWC

Mismatch between the PRC and the ARMS results in an decreased amount of carrier light coupling into the arm cavities. Critically, intensity noise on the light which is not coupled is not filtered by the arms. When coupled with a non-negligible contrast defect, this can lead to an excess coupling of intensity noise to the gravitational wave readout channel, similar to observations made in [1].

Mode matching requirements between the SRC and the ARMS are difficult to quantify because of losses[2], mode-healing[3] and mode-harming[4]. We propose that some statistical analysis/Monte Carlo simulations of slightly mismatched cavities might be a useful approach to understand and then solve any potential problem.

At the very least, the matching of the SRC cavity should have the same requirement as TCS for extraction of the GW signal:

- Combined SRC and TCS mode-matching shall maintain the extraction efficiency of the gravitational wave sidebands through the signal recycling cavity to the dark port to at least 95% of its nominal value. Squeezing will make these requirements more stringent.

A mode-matching error between the SRC and ARMS appears as an effective change in the SRM reflectivity and changes to the interferometer response to a GW signal (i.e. moves the coupled-cavity pole). This directly affects the sensitivity at high frequencies and can induce errors in the calibration of the interferometer if not properly accounted for, as reported in [2]. This is one known effect of SRC / ARM mismatch on the sensitivity curve, but we do not discount the possibilities of other effects.

Efforts are currently underway to characterize the geometry of the SRC at Hanford. An understanding of the geometries of the as-built SRCs will be very instructive when deciding whether or not SRC optic actuators are required for aLIGO and subsequent upgrades.

2.3 TCS

The original aLIGO requirements for TCS are well-summarized in [3], section 3.1.2 “Thermal Effects and the Requirements on the Thermal Compensation System and TCS Controls”. They are, briefly, summarized below:

- **Arm-cavity mode structure**: TCS shall be able to adjust the arm cavity spot size by adding up to 35 km thermal radius of curvature to all test masses HR faces.
- **RF sideband power buildup**: TCS shall compensate the thermal aberrations in the recycling cavities sufficiently that the RF sideband power in the recycling cavities does not decrease as the input laser power is increased, up to an input laser power of 120W
- **Arm cavity coupling**: TCS shall maintain the arm cavity gain to at least 95% of its nominal value.
- **Dark port power coupling**: TCS shall maintain the differential arm mismatch component of the homodyne dark port power to less than 1 mW of its nominal value.

[2]Losses: reduction of GW signal

[3]Mode-healing: injection of GW signal in HOM of one basis back into fundamental mode of SRC/OMC basis

[4]Mode-harming: injection of higher order modes without GW signal into fundamental mode

- **Gravitational wave sideband output coupling**: TCS shall maintain the extraction efficiency of the gravitational wave sidebands through the signal recycling cavity to the dark port to at least 95% of its nominal value. Since aLIGO is now in a RSE configuration, this requirement should be updated.

See also [4].

2.4 Output AWC

The output mode-matching requirements are dominated by:

- Requirements on the efficiency of transmission of GW signal to photodiodes.
- Requirements on the optical losses incurred by the injected squeezing beam.

The sensitivity improvements afforded by injecting squeezed vacuum into the interferometer drop off rapidly with the amount of loss of that squeezed vacuum field incurs. A mismatch between the mode of the squeezing field and the signal field from the interferometer result is one such source of loss. Improving the mode matching of the squeezed mode to the interferometer therefore reduces this loss and increases the sensitivity improvement achievable with squeezing. Oelker et. al. have specified 98% mode-matching for the interferometer to the OMC [5]. This will require active wavefront control. Minimizing mode matching losses in the output and squeezing injection paths in aLIGO upgrades can be considered a subcategory of the work described in the *Low loss squeezed light injection and signal readout for Advanced LIGO+* whitepaper [6]

3 Error signals

For the purposes of a discussion of error signals, it is useful to separate the role of AWC in maximising mode matching into two broad categories; static and time dependent.

3.1 Error signals for static mode mismatch

It is expected that the mode matching between several cavities may be below the required level for squeezing injection due to static errors in either the curvatures or the locations of the optics. This is especially a problem for mode matching cavities on the output side of the interferometer since the relevant beam is not available at these locations unless the full interferometer is locked. This locked state cannot be achieved unless the corner station is under vacuum, in which case access to e.g. the signal recycling cavity optics for repositioning is not available.

Since these errors are not expected to be time varying, a one-off correction or DC biasing of an actuator may be sufficient to correct them. An error signal of some form is however still required in order to determine when that error has been sufficiently corrected. In this section we discuss a few broad classes of error signal that might be considered useful for this purpose.

3.1.1 Quadratic error signals to be minimised or maximised

The static nature of several of the considered mode mismatches potentially allows for the use of signals with quadratic response to mode mismatch as useful error signals. For online corrections such signals are typically not useful due the lack of a meaningful zero crossing and the reduction in sensitivity around the working point. However, for the purposes of a one-off correction such signals may be sufficient.

One simple example for a process using one such signal would be simply to adjust the curvature or position of an optic in the power recycling cavity in order to maximize the sum of the arm cavity transmitted powers. Determining the optimal mode matching state between other cavities, especially those on the output side of the interferometer, is more complicated and requires further discussion.

3.1.2 Witness channel error signals to be held at nominal value

Such as:

- Hartmann wavefront sensors.
- Gouy phase measurements of cavities.
- Beam size sensors.

3.1.3 Direct measures of mode mismatch to be held at zero

Such as:

- Bullseye sensors.
- Dither mismatch sensing.

These are likely to be particularly useful as error signals for time-dependent mode mismatch, and so are discussed in more detail in the following section.

3.2 Error signals for time dependent mode mismatch

In order to use the available actuators to make online corrections that maximise the mode matching between cavities in the presence of time dependent wavefront perturbations, it is traditionally necessary to generate *linear* error signals for these mode mismatches. One may look to the alignment sensing and control (ASC) scheme as an example of how a range of interferometric sensors are used to provide error signals that are proportional to the relative misalignment of various cavity eigenmodes [7].

3.2.1 Bullseye sensors

One approach to the problem of AWC would be to treat it as the next order correction above misalignment: while the ASC scheme is concerned with minimising coupling between the fundamental mode and the first-order off axis mode, the AWC scheme would be concerned with minimising the the coupling between the fundamental mode and the second-order (and potentially higher) off axis modes. In this vein, the AWC sensing scheme may analogously derive useful error signals from the implementation of Bullseye sensors (BES) where the ASC scheme relies chiefly on wavefront sensors (WFS) for the generation of error signals. An experimental demonstration of a mode matching sensing and control scheme for a Fabry-Perot cavity based around such sensors was reported in [8].

3.2.2 Dither sensing

Dither sensing of mismatch is another possible option for generating linear error signals. This technique relies on the ability to dither an actuator at a frequency significantly greater than the required sensing bandwidth, however. Several of the actuators considered for implementation have low bandwidth, and so may not be suitable for application in a dither mismatch sensing scheme.

3.3 Control scheme

In terms of a control scheme, some aspects of the AWC scheme will differ from the LSC and ASC schemes to the extent that adopting the same traditional feedback approaches might not be the optimal solution for AWC. The time dependent wavefront perturbations that require correction typically occur at very low (<mHz) frequencies. Several of the mode

matching actuators under consideration also have very low bandwidth. A simple feedback loop between a sensor which measures directly the mode mismatch between two cavities and applies appropriate feedback to an actuator therefore may not be the optimal method to use for correcting the impulsive perturbations.

For these reasons it might be worthwhile to consider as an alternative a feed-forward scheme based on an experimentally measured or theoretically predicted look-up-table for the various cavity mode states as a function of an observable which responds rapidly to the impulses, such as the arm cavity transmitted power. In the case of deliberate stepping of the input power, the perturbation may even be prepared for ahead of time further minimising the time window in which the mode matching state is not optimal. The relative merits of feedback versus feedforward, or combinations of the two, should be evaluated for AWC.

3.4 Interface-specific error signals

Table 3.4 contains a list of the identified error signals for AWC. Those marked by "*to be determined*" still need to be identified. Some initial guesses at error signals that are worth investigating are listed in red text.

Interface	**Error signal description**
PSL to PMC	*to be determined* (PMC REFL/TRANS DC)
PMC to IMC	*to be determined* (IMC REFL DC)
IMC to PRC	*to be determined* (POP 18)
PRC to ARMS	Carrier optical gain of PRC (POP DC)
SRC to ARMS	*to be determined* (REFL 45 BES)
X-ARM to Y-ARM	AS port contrast defect (AS DC)
SRC to OMC	*to be determined* (AS BES 45 MHz+beacon)
SQZ to FC	*to be determined* (CCS FC REFL)
FC to SRC	*to be determined* (CCS OMC REFL)

Table 1: A list of error signals between for mode-matching at different interfaces

4 Possible Technologies

Design of the AWC actuators will be mainly shaped by the following requirements:

- **Actuation range**: how much wavefront change an actuator is required to introduce. For most actuators this will be solely a question of how much spherical power or lensing (measured in diopters) it can introduce, compared with the spherical power required to correct the expeced mismatch.
- **Actuation precision**: the smallest wavefront distortion that an actuator is required to introduce. This will prove to be less important as most actuators will struggle to provide a large actuation range but will still have a large number of steps covering their small range - leading, naturally, to a small (good) actuation precision.
- **Spatial purity**: the extent to which actuation of the device is required to introduce only the desired wavefront change. In other words, how much additional unwanted (typically higher-order) wavefront distortion is acceptable when actuating the device.
- **Spatial resolution**: the highest spatial frequency that an actuator can produce. Most problems in mode-matching in the IFO will only require spherical power, or low spatial frequencies. However, it is still necessary for us to always consider higher-order mode content requirements for AWC.
- **Bandwidth**: the maximum frequency at which the actuator can produce wavefront changes at a meaningful level.
- **Phase noise**: the requirements on an actuator in terms of phase noise contribution to the gravitational wave channel. Typically this will be dominated by vibration isolation requirements.
- **Optical loss**: the requirements on an actuator in terms of optical losses accumulated in transmission/reflection of the device. This is likely to be particularly pertinent for devices situated in the output optics path.

In this section we discuss some of the actuators that are already implemented, or in various stages of R&D.

4.1 Ring heaters

Ring heaters are an aLIGO era technology that are used to modify the optical properties of the surface and substrate of the test masses in the interferometer. They are very simple devices that apply heat to the exterior barrel of an optic [9].

Although exact configurations may change, we can fairly easily calculate an equation for the defocus of the optical path distortion induced by the RH on transmission through the substrate, D_{RH}, by calculating the temperature difference between the center and the edge of the optic and then integrating through that temperature distribution:

$$D_{RH}\left(P_{in}\right) = \frac{\frac{dn}{dT}\,P_{in}}{a\,\pi\,\left(\kappa\left(a+h\right)+4\,a^2\epsilon\,\sigma\,T_{\mathrm{env}}^3\right)}, \tag{1}$$

where P_{in} is the input power, a is the radius of the optic, h is the height, κ is the thermal conductivity, ϵ is the emissivity, σ is the Stefan-Boltzmann constant and T_{env} is the temperature of the environment. This estimate is within around 50% of the value determined by a finite-element model. For an optic size less than 1m diameter and where $h \approx a$, the defocus scales as the square of the inverse of the radius of the optic:

$$D_{RH} \propto \frac{1}{a^2} \tag{2}$$

4.2 CO_2 laser heating

CO2 lasers project an arbitrary heating pattern onto an optic to create a thermal lens. One advantage of this technique is the ability to actuate directly on higher spatial order modes. $C0_2$ laser have been used in LIGO since 2004 to heat compensation plates situated between the beam-splitter and the ITMs in order to correct for unwanted lensing in the ITM substrates [4].

4.3 Spotlight-type heaters

Originally designed for correcting errors in test mass radii of curvature in Virgo, the central heating radius of curvature corrector (CHRoCC) device utilizes ceramic heating tiles to produce infra-red thermal radiation that is projected onto the test masses. The amount of thermal radiation produced can be controlled such that the resulting heating of the substrate/coating compensates the wavefront distortion to be corrected [10]. Recent developments have focused on increasing the spatial resolution of wavefront corrections that can be made with these devices [11].

4.4 Photothermal actuator

This is an actuator that employs four ceramic heaters in thermal contact with the barrel of a transmissive optic to produce a controllable diverging lens. The conduction of the heat toward the center of the optic combined with radiative heat transfer away the plane faces sets up a radial thermal gradient which closely approximates a quadratic function. The temperature dependence of the substrate refractive index (dn/dT) and thermal expansion of the substrate generates a lens whose focal power depends on the total applied heating power [12, 13].

It has been demonstrated that SF-57 substrate can produce a lens with focal power in the range from 0 to -0.1 diopters, with little addition of unwanted higher order wavefront distortions. One useful feature of this technology is that the segmented heating system gives it the capability to correct for both symmetrical and astigmatic aberrations. One drawback may be the amount of heat that is dumped to the HAM tables when actuating the

device towards the extreme end of its range [14]. Development of this device is continuing at Syracuse University, and University of Florida where a new prototype with NiChrome heating material deposited directly on the optical barrel is being tested at the time of writing.

4.5 Thermally Deformable Mirror

This is a thermal actuator that uses an array of resistors printed on a flexible circuit board to generate controllable spatial temperature profiles inside a mirror substrate. The laser beam is incident on the AR coating, passes through the substrate, and then reflects off the HR coating (which is in thermal contact with the resistor array), finally passing once more through the substrate and back out through the AR coating. The heat supplied by the resistors controls the optical path length via the $\frac{\partial n}{\partial T}$ coefficient, (n is the index of refraction and T is the temperature). One advantage of this design is the capability to correct higher spatial frequency distortions, however its reflective design might require it to be suspended, and in-vacuum performance remains to be validated [15].

4.6 High sensitivity telescope

The High Sensitivity Telescope (HST) is a telescope with high sensitivity to the displacement of its optics. This has so far been designed to correct mismatch at the OMC with a fairly small physical actuation range. For example 10% losses overlap at OMC can be corrected adjusting the location of the lenses of about 8 mm at most [16].

It is composed by two pairs of lenses ideally located either at 45° or 135° Gouy phase apart because the mode-matching dynamic is dominated by the 2nd order transverse modes in contrast to the alignment dynamic which is dominated by 1st order transverse modes as stated in the section above. The HST design is based on the fact that the mode overlap losses due to the displacement d of a lens is inversely proportional to the Rayleigh length z_R (or equivalently to its waist size):

$$OL \approx 1 - \frac{\lambda^2}{\pi^2}\frac{d}{z_R}. \tag{3}$$

This leads to the requirement for having a small beam waist, which in turn leads informs the design choice of having two lenses close to each other. It is unlikely that only one pair of lenses is enough to provide corrections at each quadratures because the two lenses are approximatively located at same Gouy phase. A second pair of lenses might therefore be required. Advantages of this technology are the expected large dynamic range and low amount of unwanted spatial distortions. Disadvantages include the requirement for moving parts. Limitations and constrains of this technology are discussed in [17]. Further investigations on its limitations and the first implementation are underway.

5 Modeling Approach

Several tasks associated with implementing and optimizing AWC in aLIGO and beyond will benefit from simulation studies. Simulations will help to inform the design of this subsystem, as well as the commissioning when it is implemented. A preliminary picture of which different types of simulations can be useful for different aspects of AWC design and commissioning is show in tab. 5.

Simulation task	Simulation tool
Computation of requirements for mode matching between cavities	Frequency domain interferometer simulations
Design of a sensing scheme	Frequency domain interferometer simulations
Design of thermal actuators	Finite element modeling FFT optical modeling
Design and optimization of a control scheme	Time domain interferometer simulations Frequency domain interferometer simulations
Design of telescopic actuators	Ray tracing software Gaussian ABCD matrix calculations

Table 2: A rough guide as to which simulation tools will be suitable for application to which tasks in the design of AWC for aLIGO and beyond.

5.1 Computation of requirements

For computing the requirements for mode matching between cavities, several potential harmful effects of mode mismatches must be quantified. These may vary in their relative severity for different cavity mismatches, and it is likely that for any given mismatch of cavities one of these harmful effects will be the dominant effect in terms of setting the requirements for that mismatch. Requirements for mode matching between some cavities have already been laid out for aLIGO (see section 2), but in the case of some changes to the aLIGO configuration and future upgrades, these may need reassessment.

Some examples of such effects that may be taken into consideration are as follows:

- Effective squeezing losses and the impact on quantum noise level (e.g. SRC↔OMC reducing effective squeezing level).
- Loss of signal field at AS port, and corresponding quantum noise sensitivity reduction (e.g. CARM↔SRC and SRC↔OMC causing scattering of signal field to higher-order modes).
- Increased shot noise level for auxiliary degrees of freedom (e.g. IMC↔PRC and PRC↔CARM mismatch causing increased shot noise on REFL sensors).
- Increased coupling of intensity noise to the DARM channel (as observed for XARM↔YARM in e.g. LLO aLOG 14467).

- Increased coupling of intensity noise to auxiliary degrees of freedom (e.g. IMC↔PRC and PRC↔CARM causing increased coupling from intensity noise to REFL sensors).
- Changes to alignment sensing matrix (e.g. total IFO mode change causing change in Gouy phases at WFS).

Most of these effects can be modeled effectively using frequency domain interferometer simulation software, such as Finesse, MIST and Optickle.

5.2 Design of a sensing scheme

Some discussion of the generation of error signals is provided in section 3. Frequency domain interferometer simulation software will be an appropriate tool for the modeling approach for designing a mismatch sensing scheme. FFT propagation simulations may also provide useful additional capabilities here, especially for dealing with higher-order distortions and the resulting contrast defects. FINESSE [18] and MIST [19] provide the frequency domain tools here, and SIS/FOGPrime [20] and others can provide the FFT propagation tools. Recent development in FINESSE has allowed for the modeling of bullseye sensors in the context of the aLIGO interferometers (and beyond).

5.3 Design of actuators

Two broad steps are required for the design of actuators for AWC: determination of actuator requirements, and the mechanical/electrical/optical design of the actuators proper. Section 4 deals with the determination of actuator requirements. This process will depend in the first steps on the results of simulation studies into the requirements for the wavefront matching between different cavity interfaces. In terms of the design of the actuators themselves, several simulation approaches may be useful.

For thermal actuators such as ring heaters, CO_2 laser heating, small thermal lensing elements or IR heat projection devices, finite element modeling is likely to be the most useful tool for determining a design which can fulfil the requirements. Analytical modeling may also play an important role here. Time domain simulations can provide useful information about the bandwidth of such devices.

For telescopic devices, such as movable lenses or mirrors, ray tracing software may be the most useful tool. For compact telescope designs, astigmatic and spherical aberrations can be particular concerns which may be evaluated and mitigated by using designs informed by ray tracing software.

5.4 Design and optimization of control scheme

With a well defined sensing scheme and a range of actuators capable of correcting mismatches, a scheme is required for connecting the two together in order to maintain an optimal interferometer working point. Due to the long time constants of both the expected wavefront distortions and some of the proposed actuators, a typical control scheme design such as those

for LSC and ASC may not be the only, or optimal, solution for this task (as discussed briefly in section 3). As such, it may be worth considering the use of time domain simulations such as E2E [21], perhaps in combination with state-space models for thermally driven optical components, as well as frequency domain models.

6 Institutions

- California Insitute of Technology: designed thermal compensation system for aLIGO. Continuing modeling work for determining requirements on output/squeezing beam mode matching.
- University of Florida: helped test RH for aLIGO. Designed alternative ring heater design and photothermal acutator. Continuing involvement in modeling work for determination of mode matching requirements, sensing schemes and control.
- Syracuse University: continuing development of UF photothermal actuators. Developing high-sensitive telescope and closed loop mode matching feedback experiments.
- University of Adelaide/ANU: designed/provided Hartmann wavefront sensors for aLIGO. Characterizing as-built signal recycling cavities.
- Massachusetts Institute of Technology: developing squeezing source, filter cavity and squeezing injection optics for aLIGO.
- University of Birmingham: simulation support for determining AWC requirements, sensing and control schemes in aLIGO and beyond.

Bram and I chatted and we thought understanding the modematching through the signal recycling mirror would be a good thing to focus our efforts on. The first thing that we are doing in this regard is trying to really measure the as-built SRC at LHO. Ellie is doing a series of measurements to try and quantify this. These include measuring the length and trying to accurately determine the as-built-Gouy Phase (Not so easy). I hope that once this has been achieved we will be able to work with Paul to try develop a complete model of the as-built SRC and its impacts on future upgrades. I think this partial answers your question in Section 3 of LIGO-T1400715-v3.

7 Timeline

- Determine the critical noise couplings that drive the requirements for mode matching at all interfaces - by fall/winter 2015.
- Derive requirements for mode matching at all interfaces, and corresponding actuator requirements - by winter 2015.
- Derive mode matching sensing scheme appropriate for use in aLIGO and beyond - by fall/winter 2015.
- R&D on optimization of control schemes for online correction of time dependent mode mismatches - ongoing.
- Choose appropriate actuators for further development and integration in aLIGO and beyond - by spring 2016.
- Install additional mode matching sensors and actuators - fall/winter 2016.

8 TCS Review

8.1 TCS Review

TCS, in a general sense, can do the following:

1. Match the two IFO arms together. Both in the FP cavities and short Michelson. Minimizing the contrast defect. This moves from Figure 1 to Figure 2.
2. Match the common arms to ONE of the recycling cavities (either PRC or SRC). This moves from Figure 2 to Figure 3.

TCS *cannot* currently mode-match both arms to each other *and* match to the PRC and SRC simultaneously. This is illustrated schematically in the following figures.

8.2 TCS History

The adaptive optics required for TCS are, likely, the most stringent due to the fact that the test masses are the source of the largest continuous variation in wavefront throughout the whole interferometer.

TCS, amongst other things, should minimize the contrast defect between the arms (reduce the load on the OMC). Actuate on higher order modes.

- PRC to IFO (common mode TCS)
- IFO to SRC (differential mode TCS)

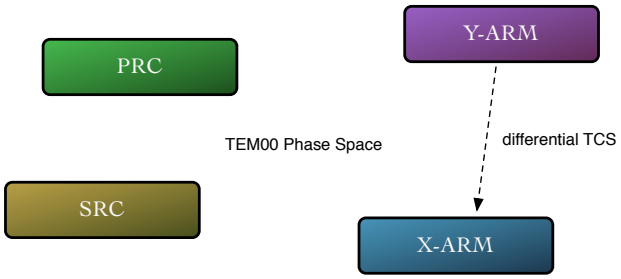

Figure 1: TCS - Stage 0: The eigenmodes of all four cavities occupy different points in the phase space of spatial modes. Differential mode TCS should be applied.

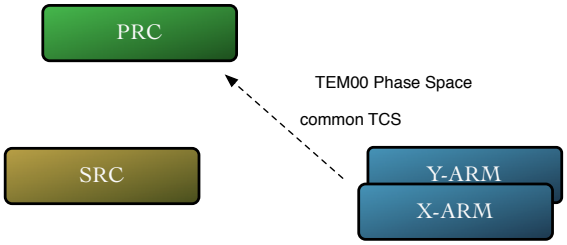

Figure 2: TCS - Stage 1: TCS was used to drive the arm cavity modes together to minimize the differential mode (contrast defect). Common mode TCS should be applied from here.

A Mode matching as an invariant

The overlap integral between two Gaussian beams that have slightly different beam sizes and defocus (inverse of ROC) is given by:

$$OL \approx 1 - \left(\frac{\Delta w}{w}\right)^2 - \left(\frac{w^2\,\Delta S\,k}{4}\right)^2 \tag{4}$$

where Δw is the difference in beam size and ΔS is the difference in the defocus. The first term in parentheses is the fractional difference in beam size squared. The second term is the differential phase change at the beam radius over root two, all squared, i.e,

$$\frac{w^2\,\Delta S\,k}{4} = 2\,\pi\,\frac{ds_{w2}}{\lambda} \tag{5}$$

where ds_{w2} is the sagitta at beam radius of $w/\sqrt{2}$.

The overlap between two beams is independent of the plane at which this is calculated. In other words, provided the two beams are propagated to the same plane, the values of Δw,

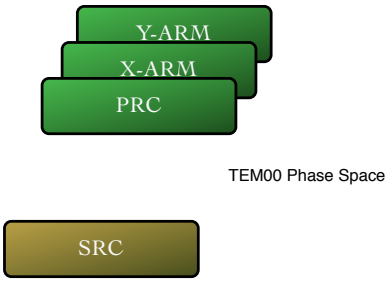

Figure 3: TCS - Stage 1: TCS was used to drive the common arm cavity mode to maximize the overlap with ONE of the recycling cavity modes - in this case, the PRC (build-up). At this point, there are no actuators exist to move the PRC and SRC modes together.

w and ΔS will vary such that OL is unchanged. As such, the beams can be propagated to the most convenient plane to calculate the overlap.

References

[1] D. Martynov, LLO aLOG 14736, "Input RIN coupling, arm losses", 09.21.2014, https://alog.ligo-la.caltech.edu/aLOG/index.php?callRep=14736

[2] G. Vajente, LIGO-G1500641, "Simulation of SRCL coupling to DARM and DARM pole frequency", 05.13.2005, https://dcc.ligo.org/G1500641

[3] M. Smith, P. Willems, LIGO-T000092-v4, "Auxiliary Optics Support System Design Requirements Document, Vol. 1: Thermal Compensation System", 09.16.2014, https://dcc.ligo.org/LIGO-T000092.

[4] S. Ballmer *et al.*, LIGO-T050064, "Thermal Compensation System Description", 05.10.2005, https://dcc.ligo.org/DocDB/0027/T050064/000/T050064-00.pdf.

[5] E. Oelker, L. Barsotti, S. Dwyer, D. Sigg, N. Mavalvala, "Squeezed light for advanced gravitational wave detectors and beyond", *Optics Express*, **22**, 21106-21121 (2014), http://www.opticsinfobase.org/oe/abstract.cfm?uri=oe-22-17-21106

[6] L. Barsotti, LIGO-T1400715, "Low loss squeezed light injection and signal readout for Advanced LIGO+", 04.01.2015, https://dcc.ligo.org/LIGO-T1400715.

[7] L. Barsotti, LIGO-T0900511, "Modeling of Alignment Sensing and Control for Advanced LIGO", 10.19.2009, https://dcc.ligo.org/T0900511

[8] G. Mueller, Q.-Z. Shu, R. X. Adhikari, D. B. Tanner, D. Reitze, D. Sigg, N. Mavalvala, and J. Camp, "Determination and optimization of mode matching into optical cavities by heterodyne detection", *Optics Letters*, **25**, 266-268 (2000).

[9] C. Zhao *et al.*, "Compensation of Strong Thermal Lensing in High-Optical-Power Cavities", *Physical Review Letters*, **96**, 231101 (2006).

[10] A. Chiummo, LIGO-G1101106, "Radius of Curvature Correction (CHRoCC)", 09.28.2011, https://dcc.ligo.org/LIGO-G1101106

[11] R. A. Day, G. Vajente, M. Kasprzack, and J. Marque, "Reduction of higher order mode generation in large scale gravitational wave interferometers by central heating residual aberration correction", *Physical Review D* **87**, 082003 (2013).

[12] M. A. Arain, W. Z. Korth, L. F. Williams, R. M. Martin, G. Mueller, D. B. Tanner, and D. H. Reitze, "Adaptive control of modal properties of optical beams using photothermal effects", *Optics Express*, 18:2767 (2010), https://www.osapublishing.org/oe/fulltext.cfm?uri=oe-18-3-2767&id=195231.

[13] Z. Liu, P. Fulda, M. A. Arain, L. Williams, G. Mueller, D. B. Tanner, and D. H. Reitze, "Feedback control of optical beam spatial profiles using thermal lensing", *Applied Optics*, **52**, 26, 6452-6457 (2013), https://www.osapublishing.org/ao/abstract.cfm?uri=ao-52-26-6452.

[14] P. Fulda, R. Goetz, G. Mueller, D. B. Tanner, LIGO-G1401024, "Active thermal lenses for mode matching in aLIGO", 08.25.2014, https://dcc.ligo.org/LIGO-G1401024.

[15] M. Kasprzack, B. Canuel, F. Cavalier, R. Day, E. Genin, J. Marque, D. Sentenac and G. Vajente, "Performance of a thermally deformable mirror for correction of low-order aberrations in laser beams", *Applied Optics*, **52**, 12, 2909-2916 (2013), https://www.osapublishing.org/ao/abstract.cfm?uri=ao-52-12-2909.

[16] A. Brooks, A. Perreca, L. Barsotti, P. Fulda, LIGO-G1500372, "Active Wavefront Control, or the story of ADaptive Higher Order Mode Control (ad HOC)", 03.31.2015, https://dcc.ligo.org/LIGO-G1500372.

[17] A. Perreca, F. Magana-Sandoval, S. Ballmer, LIGO-G1401051, "Advanced Ligo: Adaptive Mode Matching for the Output Mode Cleaner", https://dcc.ligo.org/LIGO-G1401051

[18] A. Freise, G. Heinzel, H. Lück, R. Schilling, B. Willke, and K. Danzmann, "Frequency-domain interferometer simulation with higher-order spatial modes" *Class. Quantum Grav.*, **21**, S1067 (2004), the program is available at http://www.gwoptics.org/finesse.

[19] G. Vajente, LIGO-G1400322, "MIST", 03.18.2014, https://dcc.ligo.org/LIGO-G1400322.

[20] H. Yamamoto, LIGO-G080084, "AdvLIGO Static Interferometer Simulation", 02.11.2011, https://dcc.ligo.org/LIGO-G080084.

[21] H. Yamamoto, LIGO-G070658,"e2e - LIGO end to end time domain simulation", 02.10.2011, https://dcc.ligo.org/LIGO-G070658.